#### PULSE-WIDTH-AMPLITUDE MODULATION (PWAM) FOR REDUCING INVERTER SWITCHING LOSS IN HEV/EV MOTOR OR GENERATOR SYSTEM

By

Xianhao Yu

#### A THESIS

Submitted to
Michigan State University
in partial fulfillment of the requirements
for the degree of

MASTER OF SCIENCE

**Electrical Engineering** 

2012

#### **ABSTRACT**

#### PULSE-WIDTH-AMPLITUDE MODULATION (PWAM) FOR REDUCING INVERTER SWITCHING LOSS IN HEV/EV MOTOR OR GENERATOR SYSTEM

By

#### Xianhao Yu

Ideally the power converters are supposed to be lossless. However in the real world there are many reasons that can cause power loss in the power converter system. Therefore minimizing the power loss and operating system at high efficiency point is an essential step towards developing optimized power conversion system.

This thesis introduces a novel PWM control strategy – "Pulse-Width-Amplitude Modulation (PWAM)" method for HEV/EV motor or generator system. This modulation method is quite different from other PWM methods that have been well researched or commonly used for the inverter in HEV/EV system. By using this method, only one phase leg of the inverter is doing switching action at any time. Therefore, the inverter total switching time is reduced to one third comparing with conventional SPWM method and the total switching loss can be reduced by at least 50% or even more depending on the load condition (power factor). In addition, the inverter dc-link requires much smaller capacitor when PWAM method is applied, which makes the system smaller size and lighter weight. Simulation and experimental results are provided to verify inverter efficiency improvement.

Dedicated to my Father and Mother: Shengwei Yu and Fulan Zhao

#### **ACKNOWLEDGEMENTS**

I would like to give my heartfelt thanks to my dear advisor, Dr. Fang Z. Peng. It is you who offer me the opportunity to come to US for a higher education. It is also you who taught me and helped me on every aspects of my life. I will treasure what I learned from here and never forget the experience that I stayed in the Power Electronics and Motor Drive Lab.

I also want to thank the people I met in Dr. Peng Lab – Dr. Baoming Ge, Dr. Xi Lu, Dr. Dong Cao, Dr. Shuai Jiang, Dr. Qin Lei, Dr. Craig Rogers and many others. You are all talent and hardworking, which set good example for me. I learned a lot from you.

### TABLE OF CONTENTS

LIST OF TABLES vi				
LIST (	OF FIGURES		vii	
СНАР	TER 1 Introduction.		1	
1.1	Background-PWM	Inverters	1	
1.	.1 Inverter Applcati	tions	3	
1.2	Topology		5	
1.3	PWM Method and Sv	witching Loss	6	
1.4	Resomant DC Link		9	
1.5	Outline of Thesis		10	
СНАР	TER 2 PWAM Contr	trol Method	11	
2.1	Background - Single	e-Phase PWM Method	11	
2.2	Operating Principle		13	
СНАР	TER 3 System Power	er losses Analysis	17	
3.1	Inverter Switching Lo	oss	17	
3.2	Inverter Conduction l	Loss	21	
СНАР	TER 4 Experiment R	Result	22	
4.1	Experiment Setup and	nd Result	22	
4.2	System Modifications	ns	26	
СНАР	TER 5 Conclusion ar	and Future Work	30	
5.1	Contributions		30	
5.2	Future Work		30	
Ribling	ranhy		32.	

# LIST OF TABLES

Table I.	System specification for	or experiment	24
----------	--------------------------	---------------	----

# **LIST OF FIGURES**

Figure 1.1 PWM voltage source inverter: (a) single-phase inverter, (b) 3-phase inverter	. 2
Figure 1.2 Solar inverter system	. 4
Figure 1.3 Toyota Prius powertrain system configuration	. 4
Figure 1.4 The boost converter - inverter system topology for PWAM method	. 6
Figure 1.5 Switching transition and losses (For interpretation of the references to color in the and all other figures, the reader is referred to the electronic version of this thesis	s)
Figure 1.6 Space Vector PWM (SVPWM) method	. 9
Figure 2.1 Single-phase PWM system configuration	11
Figure 2.2 Inverter switching pattern based on three phase voltage references relationship 1	14
Figure 2.3 System equivalent circuit for the condition of "Va>Vb>Vc"	14
Figure 2.4 PWAM simulation (P.F.=1)	16
Figure 2.5 PWAM simulation (P.F.=0.87)	16
Figure 3.1 The relationship between power loss and load power factor	19
Figure 3.2 Switching loss comparison between PWAM and SPWM	20
Figure 4.1 Boost converter –inverter system prototype	23

Figure 4.2 DC-link waveform and IGBT voltage waveforms in three phase legs	25
Figure 4.3 DC-link waveform and 3-phase output line-to-line voltage using PWAM at 1 kW	25
Figure 4.4 Efficiency curves of PWAM and SPWM	26
Figure 4.5 System PCB layout modification: (a) first version; (b) second version	28
Figure 4.6 Version comparison picture	29

# **CHAPTER 1 Introduction**

### 1.1 Background – PWM Inverters

An inverter is the type of power electronics system that converts direct current (DC) to alternative current (AC). The input of it is connected to DC power source, such as batteries or PV panels, and the out put of the inverter is designed to supply AC power at a desired voltage and frequency.

One type of inverter is called voltage-fed inverter (VFI) or voltage-source inverter (VSI) if the input voltage is fixed, while the other type is called current-fed inverter (CFI) or current-source inverter (CSI) if the input current remains constant. Comparing with current-source inverter, the voltage-source inverter is more popular and widely applied in both research field and industry. For the voltage-source inverter whose input voltage is fixed, its output voltage level can be controlled by varying the inverter's gain and normally the approach is using pulse-width-modulation (PWM) control [1].

There are two basic topologies for PWM voltage source inverter that are shown in figure 1.1. One is single-phase inverter and the other is three-phase inverter. The single-phase inverter has four switching devices and the AC current passes through the single load, while the three-phase inverter consists of 6 switching devices that generate 3-phase AC currents. It is clear to see from the topologies that the major components of inverters are those high-speed semiconductor switching devices, which are denoted as S1, S2, S3 and S4 in the figure. Depending on different

power ratings and applications, different devices such as MOSFET and IGBT can be selected to fulfill the functions.

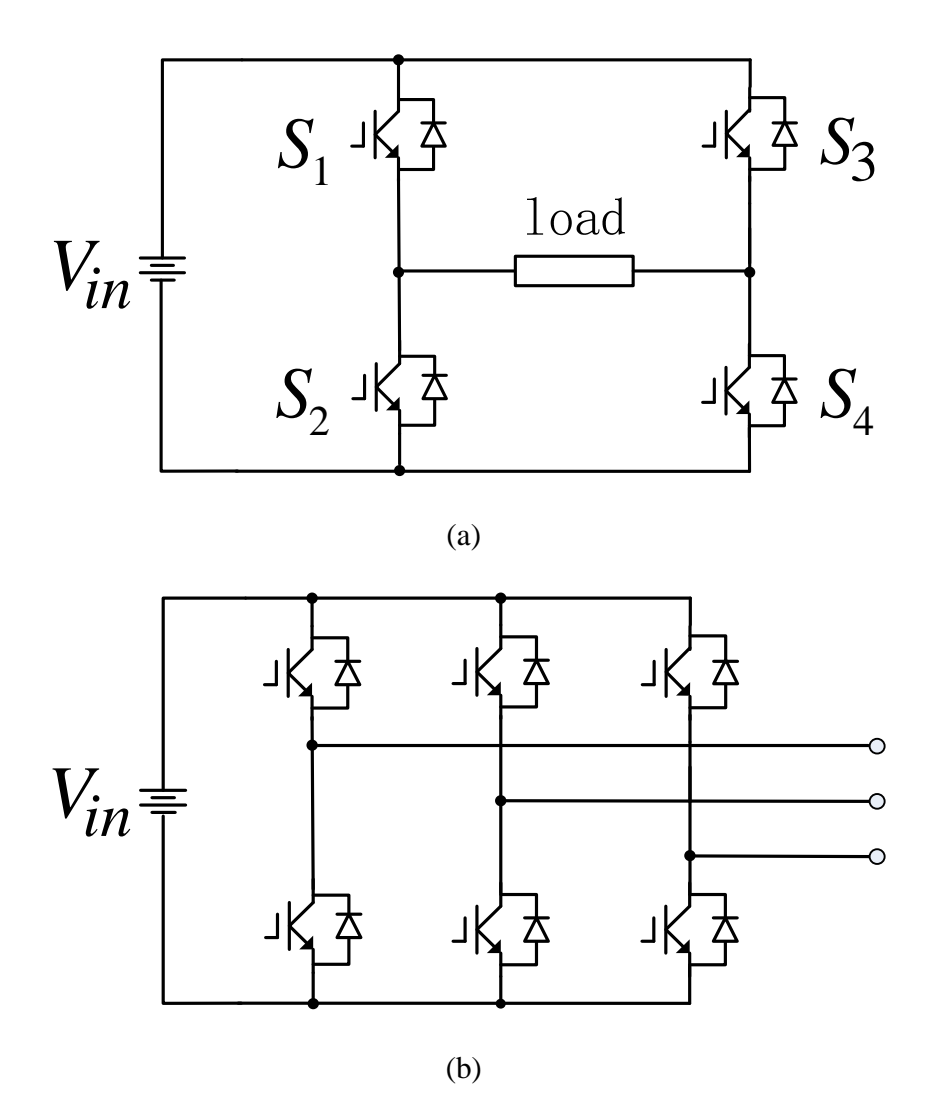


Figure 1.1 PWM voltage source inverter: (a) single-phase inverter, (b) 3-phase inverter.

#### 1.1.1 Inverter Applications

Inverters are widely used in many different applications:

- DC power source utilization,
- Uninterruptable power supply,
- Electric motor drive
- VHDC transmission line
- Induction heating
- Air conditioning

The list only provides some of the examples of inverter application. The solar inverter system and the electric vehicle motor drive system are introduced here in detail.

Solar power is one type of renewable energy that is considered as a really good replacement of fossil fuel. The solar panel was invented and produced to accomplish the solar energy conversion. It turns the optical energy into electric energy, which is in the form of the DC electricity. Then the solar inverter system finishes the energy harvesting process and injects the power into power grid. Figure 1.2 demonstrates the system configuration of this kind of system. A DC-DC converter is needed here to control the power flow and also provide a stable voltage for dc-link. The inverter is supposed to generate the 3-phase voltage following grid's voltage amplitude and frequency.

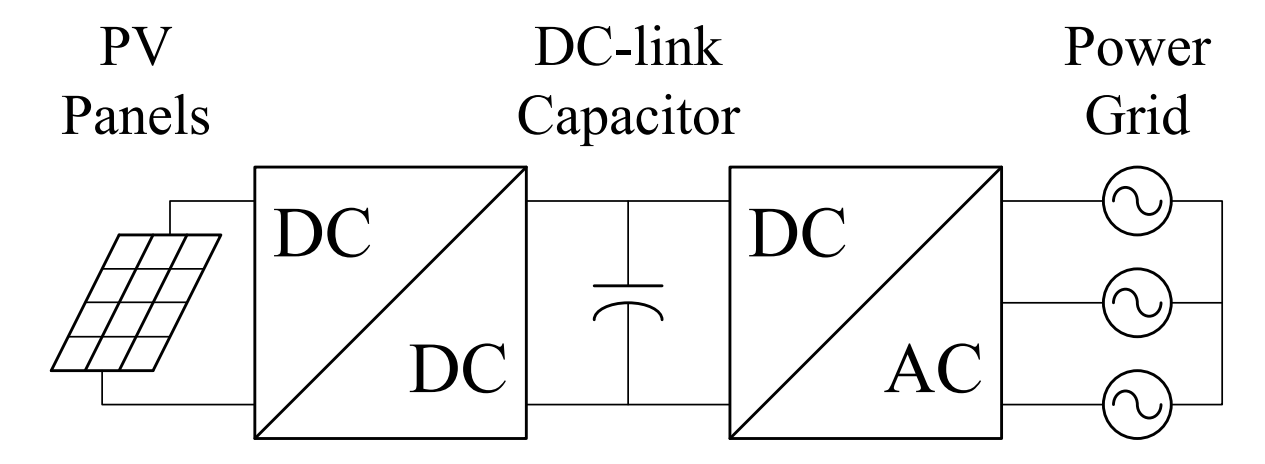


Figure 1.2 Solar inverter system

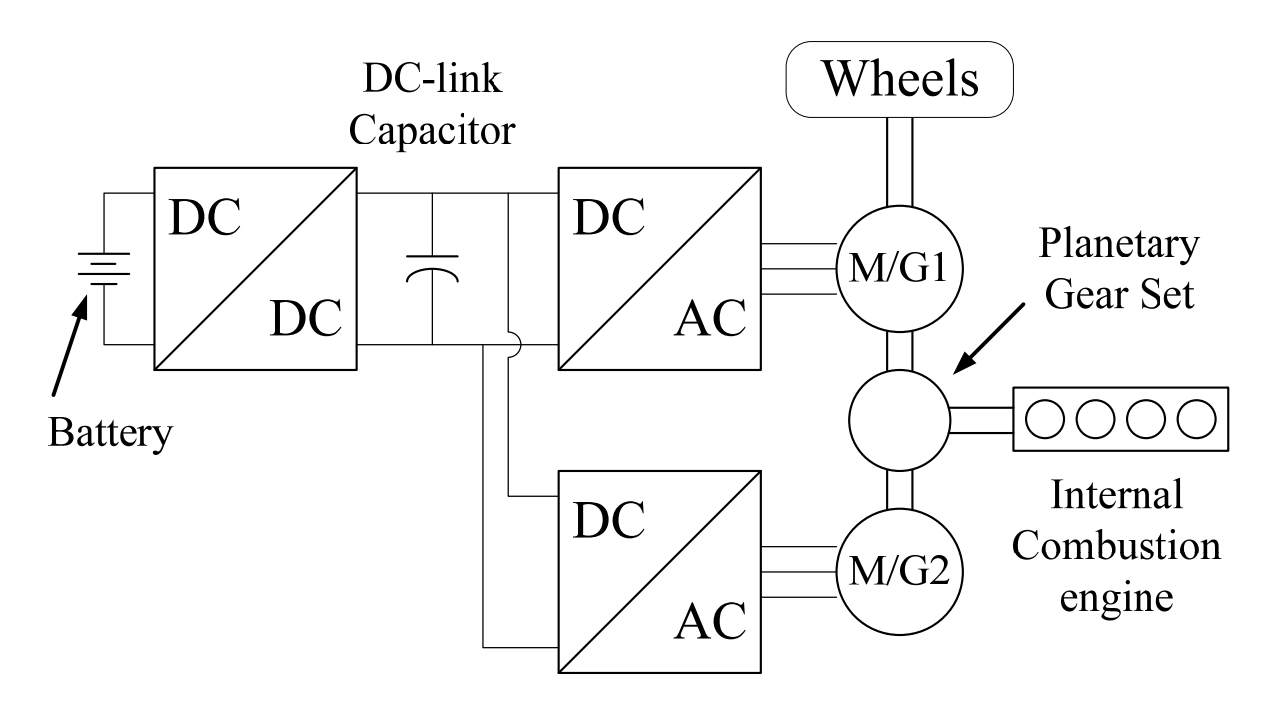


Figure 1.3 Toyota Prius powertrain system configuration

Hybrid Electric Vehicle (HEV) and Electric Vehicle (EV) are playing more important role in the auto industry nowadays. Instead of relying on the conventional fossil fuel powered vehicles, these new types of vehicles offers people an alternative of using different energy sources to drive. Moreover, the efficiency of energy utilization in HEV/EV system is much higher than conventional vehicle. Figure 1.3 shows the power electronics parts and vehicle power train of the Toyota Hybrid Prius, which is a parallel hybrid system. There are two inverter systems that drive two motors separately. The inverters are designed for bidirectional power flow and the motors could work as generators as well.

Since the internal combustion engine should only run under the most efficient operating point and provide large power at high speed, it will not be activated all the time. The top inverter controls the motor/generator 1 to drive the wheels directly for low speed navigation. When engine is running at high speed, an extra part of power could be send back to battery through motor/generator 2 and the bottom inverter. During breaking operation, the energy collected from wheels is transferred back to battery through motor/generator 1 and the top inverter.

## 1.2 Topology

This thesis focus on a very simple but very wildly used topology for control method analysis. Figure 1.4 shows the boost converter – inverter system, which consist of a DC/DC boost converter and a simple three-phase PWM voltage source inverter. Generally, a large capacitor is installed on the dc-link between boost converter and inverter. This is because an ideal dc source is expected at the input side of inverter. If there is not a battery on the dc-link, the big capacitor is required to store enough energy and absorb the current ripple.

Many applications that have been mentioned previously use this topology, including HEV/EV system. In HEV/EV system, a battery is needed to provide and to restore the power. The DC/AC inverter is used to convert dc power on the dc-link into AC power so that it can drive the electric motor/traction motor. During regenerative mode, the motor could also run as a generator and inverter should be able to transfer the power back from the AC to DC side. For most of the time, a DC/DC converter is also installed in the system between battery and inverter to boost battery voltage to match the dc-link voltage.

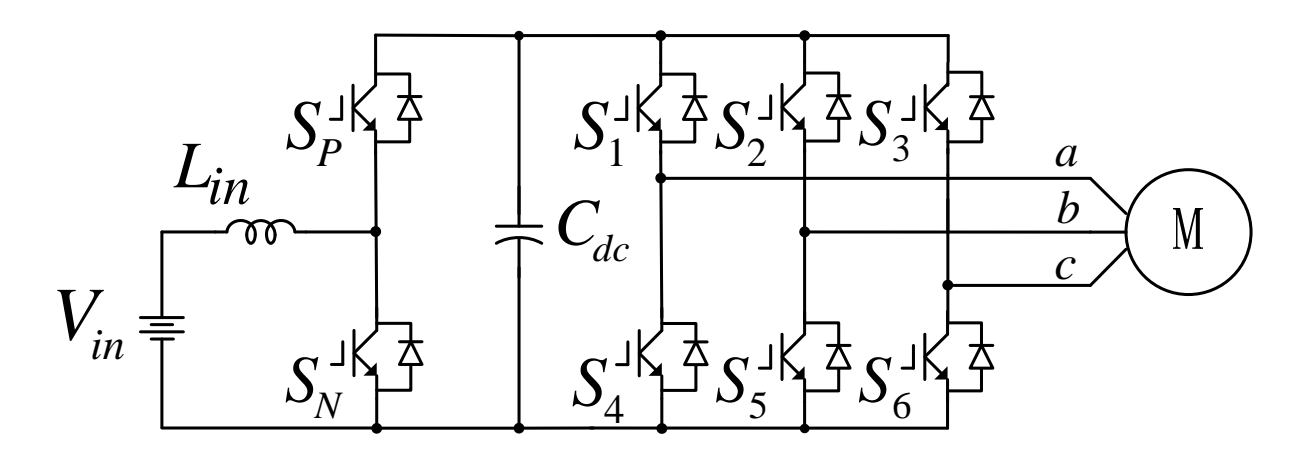


Figure 1.4 The boost converter – inverter system topology for PWAM method

## 1.3 PWM Method and Switching Loss

Since high efficiency is essential goal that HEV/EV pursuit, how to reduce power losses for the whole system is always an important factor within design consideration. Switching loss is one part of the major power losses from operation of the inverter system. Figure 1.5 shows the device's voltage and current waveforms during the switching transition, which explains how switching and conduction losses generate.

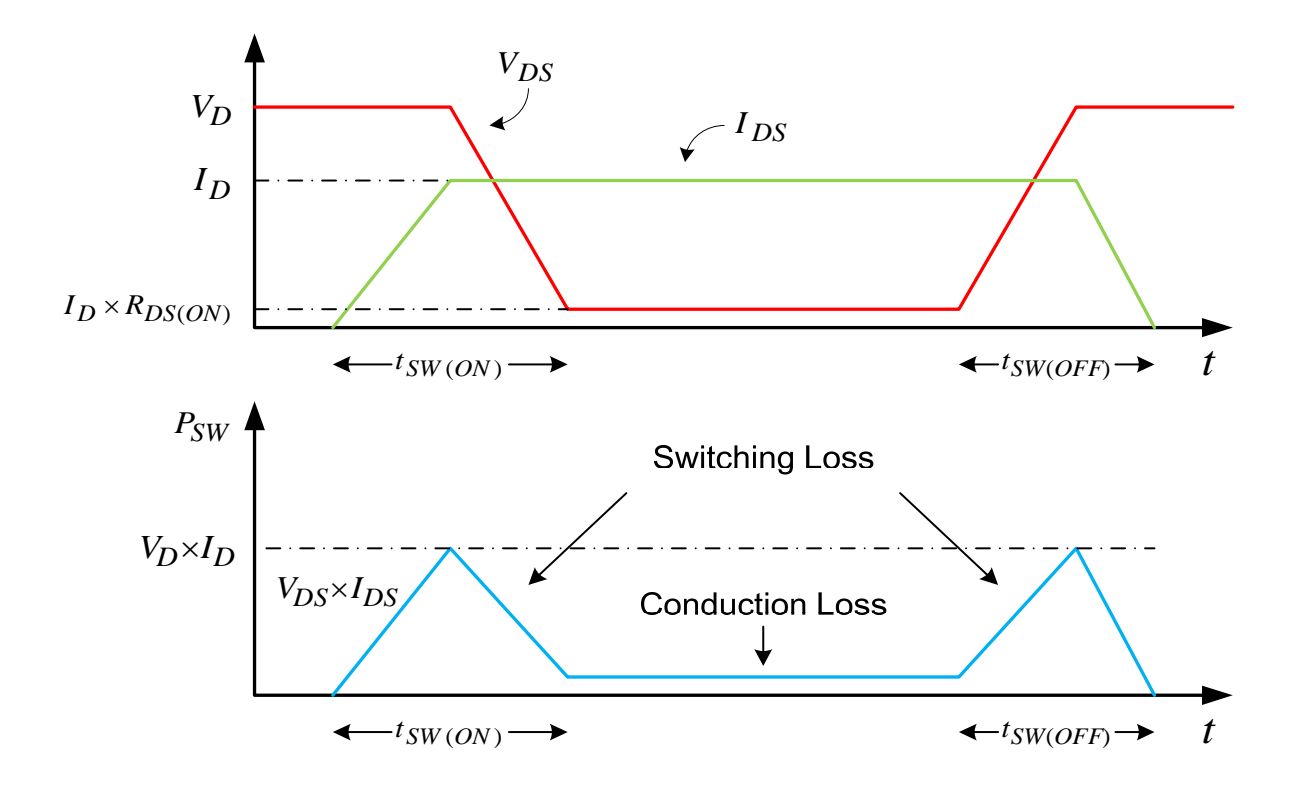


Figure 1.5 Switching transition and losses [2]

(For interpretation of the references to color in this and all other figures, the reader is referred to the electronic version of this thesis)

To reduce switching loss, one method is to reduce to the area of the current-voltage integral. From figure 1.5, the switching loss is calculated by integrated the instantaneous voltage across the switching device and the current passing through it. The size of the area is can be reduced is the switching transition is shortened. Moreover, the area can be completely removed if instantaneous current or voltage is zero during transition, which is known as Zero Voltage/Current Switching (ZVS/ZCS).

Another approach to reduce switching loss is preventing the switching action from happening. In this case, the switching transition in figure 1.5 will not even occur. Therefore switching loss is not an issue any more. Many different Pulse-Width-Modulation (PWM) methods have been proposed to achieve switching loss reduction in this way.

For the inverter system in HEV/EV, there are many modulation methods that are developed and analyzed to reduce switching loss. The conventional space vector PWM (SVPWM) strategy was proposed in [3] in order to extend the linear modulation range. To generate the reference voltage vector, as showed in figure 1.6, one can find any combination by utilizing the six active switching states and two zero switching states. A good switching combination can reduce the switching instance in each carrier cycle. Switching loss by using SVPWM is then reduced by roughly 13% over conventional Sinusoidal PWM (SPWM) [11], while waveform quality degrades at high modulation index [4]-[6]. Discontinuous PWM (DPWM) methods were developed mainly for reducing the switching loss via completely stop switching action for a certain period of time (commonly 60 or 120 degrees of the fundamental period). By injecting a zero sequence signal, the new three phase references are clamped to the positive or negative dc link instead of following sinusoidal waveform. Controller is not sending any PWM switching signals for this period of time to turn on or turn off the devices. Consequently, the DPWM method reduces the number of switching instances by up to one third of the fundamental period, thus reducing switching loss. Also, switching loss reduced by DPWM methods depend on the load power factor [7]-[10]. Six-step operation is another modulation method that fully uses the dc voltage and requires very few switching instances. The switching loss can be reduced by half compared to SPWM [12]. However, for six-step operation, the motor will experience great loss and torque ripple due to bad output waveform quality.

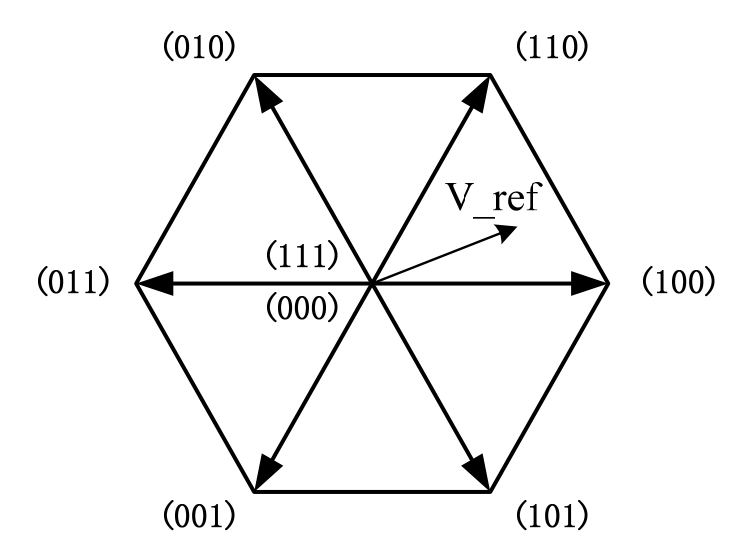


Figure 1.6 Space-Vector PWM (SVPWM) method

### 1.4 Resonant DC Link

The idea of "resonant dc-link" is also utilized for reducing converter's switching loss [13]. Unlike the all the PWM control method mentioned in the last section, the number of times of switching action is not changed or modified. Lossless switching is achieved by applied zero voltage switching technique here [14].

The switching loss comes from the integration of product of voltage across the device and the current pass through it during switching transient. If either the voltage or current decreases or disappears, switching loss will decrease accordingly. In the case of resonant dc-link, the converter does not have fixed dc-link voltage; instead it has dc-link voltage that varies with the switching action. When the dc-link voltage is controlled to reach zero at switch turning-on / turning-off transition, the voltage across device will be zero, integration of switching loss will then be zero [15].

This thesis is trying to use novel PWM method to reduce switching loss. Although zero voltage switching technique is not adopted to improve efficiency, another feature of resonant dc-link has been noticed – the big dc-link capacitor in conventional inverter system is not needed anymore with a fluctuated dc-link [16].

## 1.5 Outline of Thesis

This paper introduced a novel control strategy – Pulse-Width-Amplitude Modulation (PWAM) method for HEV/EV motor drive system. The original idea is from single phase PWM control method that was proposed in [17] and [18] for grid-connected inverter system. Unlike the case in [17] and [18], however, PWAM method for motor drive has to consider the situations of varied power factor and output frequency, which is more complicated. By using this method, only one phase leg of the inverter is doing switching action for every PWM-carrier period. Therefore, the inverter total switching time is reduced to one third comparing with conventional SPWM method. and the total switching loss can be greatly reduced by at least 50% or even more depending on the load power factor. In addition, the inverter dc-link requires much smaller capacitor when PWAM method is applied, which makes the system smaller size and lighter weight. A 1 kW boost converter inverter system prototype was built to test the system efficiency with conventional SPWM method and PWAM method. Theoretical power loss analysis, simulation and experimental results are provided to verify inverter efficiency improvement.

.

# **CHAPTER 2 PWAM Control Method**

In this chapter a new PWM control strategy is introduced. Unlike those conventional pulse-width modulation control method that only modulate the pulse width of the control signals, the new method also deals with the amplitude of control signals. So it can be named as "Pulse-Width-Amplitude Modulation (PWAM)" method.

## 2.1 Background – Single-Phase PWM Method

To understand how PWAM method works, introducing Single-Phase PWM Method would be a good start. Single-Phase PWM method was proposed by a Japanese researcher Hideaki Fujita for the application of solar inverter system. It uses the same topology which consists of a boost converter and a three phase inverter. The input of the system is connected to solar panels, which generates dc voltage and current. After step up the dc voltage to a higher level by boost converter, the inverter is installed to inject electric power into power grid in the form of three phase ac voltage and ac current. Figure 2.1 shows the system configuration of Single-Phase PWM method.

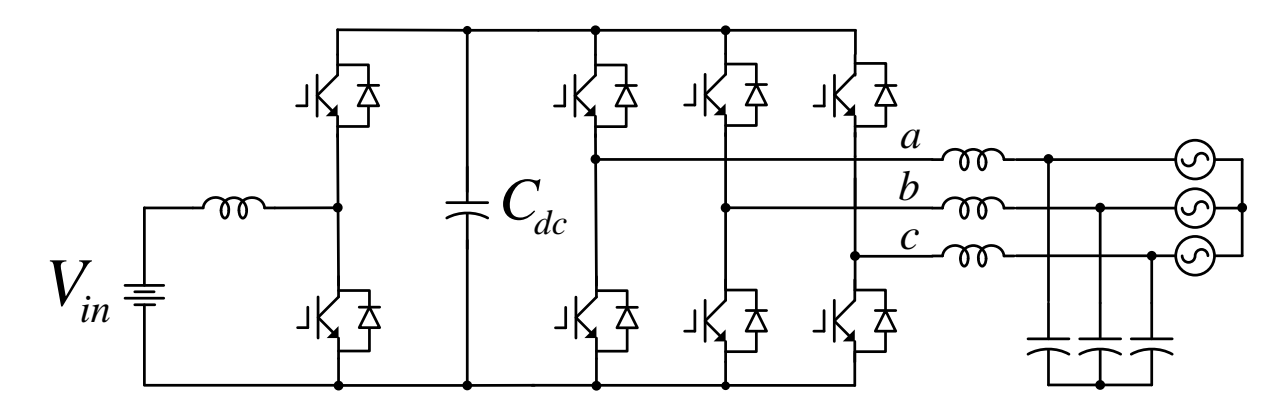


Figure 2.1 Single-phase PWM system configuration

Single-Phase PWM method was proposed to reduced inverter switching loss. There are always two phase legs of the inverter that don't need have any switching action (keep on or off) for two third of the fundamental period, and only one phase leg operating PWM switching action for any moment. The total switching time was then reduced by two third, therefore the switching loss was greatly reduced.

There are a few points that needed to be noticed for this method. First, this is a grid connected application, and the load of the inverter could be assumed as an idea load with 50-Hz frequency and idea 200-V voltage. The dc link voltage of the inverter is clamped by the power grid line-to-line voltage because the switches of inverter keep turning on and off for a long period of time. The relationship of the dc link voltage and the three phase line-to-line voltage is the same as the case of three phase diode rectifier, which is

$$V_{dc} = \frac{3\sqrt{2}}{\pi} V_{ll(rms)}$$

The formula gives average dc link voltage value, but there is small voltage ripple on which has the six times of fundamental frequency. With this expected ripple that appears on the inverter dc link, it is not necessary to have really large capacitor to clamp voltage at a fixed value. This is reason the Single-Phase PWM not only reduces inverter switching loss, but also reduces the dc-link capacitance.

Another point is that the boost converter in Single-Phase PWM application was controlled based on the power which would be transferred through this system. The reference of power rating is the only thing important for controlling the boost converter. This is different from the PWAM control method and will be explained in the later section.

## 2.2 Operating Principle

At steady state, the motor drive is running at a desired condition, so the inverter has to generate output with expected voltage and frequency values. By setting the expected values as references, PWAM method can be applied. Figure 2.2 shows the three phase output references and the inverter switch pattern.  $S_a$ ,  $S_b$  and  $S_c$ , represent the upper switches of three inverter phase  $\log a$ ,  $\log a$ , and  $\log a$ , respectively. Let the case " $\log a$ 0" be an example. When the phase  $\log a$ 1 voltage is larger than the other two phase voltages, upper switch in phase  $\log a$ 1 gets turned on all the time, denoted as "1". At the same time, phase  $\log a$ 2 voltage is the smallest. Upper switch in phase  $\log a$ 3 leg is set to be off all the time, denoted as "0". This means the lower switch in phase  $\log a$ 3 leg is turned on. Only phase  $\log a$ 4 leg in this case is doing PWM switching action, denoted as "\*". Therefore, using this method, only one phase  $\log a$ 4 the inverter is doing switching action for every PWM-carrier period. Figure 2.3 shows the system equivalent circuit at this moment. It is easy to see that the output line-to-line voltage  $\log a$ 5 leg.

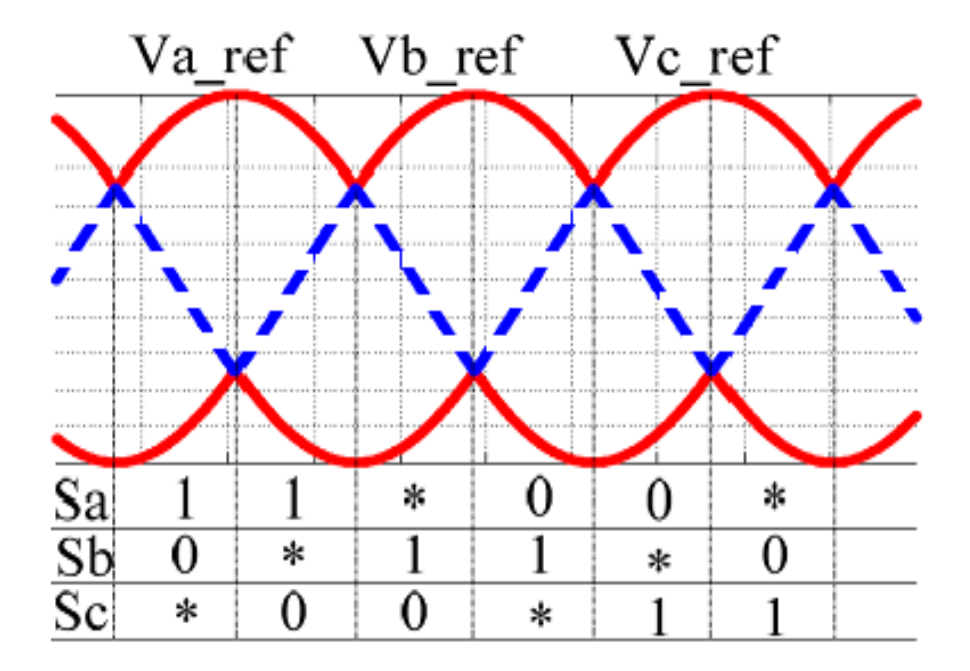


Figure 2.2 Inverter switching pattern based on three phase voltage references relationship

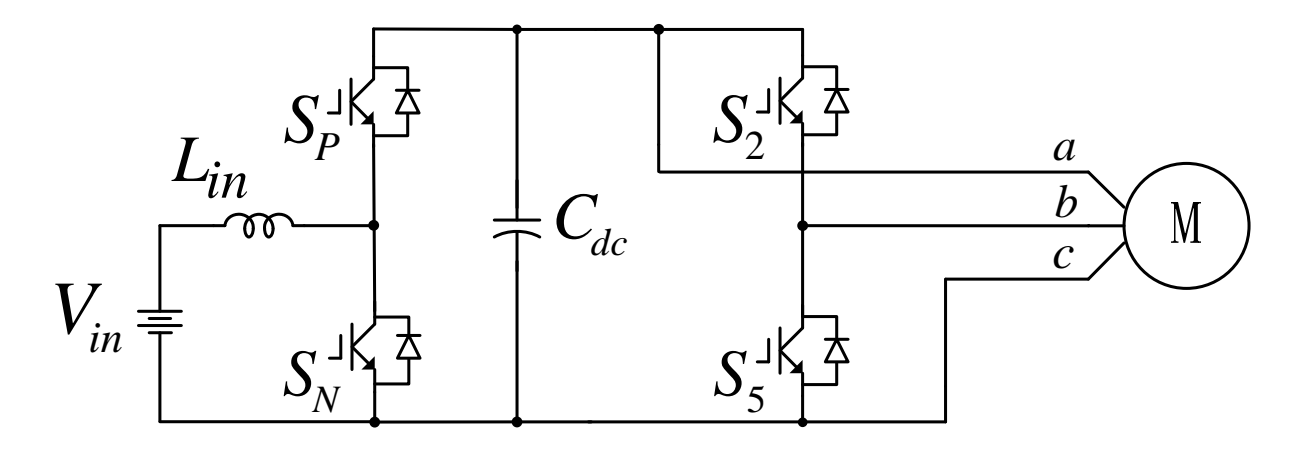


Figure 2.3 System equivalent circuit for the condition of "Va>Vb>Vc"

In PWAM control, dc-link voltage has to vary with a voltage ripple whose frequency is six times of output frequency. This kind of ripple is called  $6\omega$ . The peaks of the ripple are corresponding to the peaks of output three phase line-to-line voltage. In order to generate this ripple, the boost converter needs to be controlled. The equation of voltage gain for boost converter is

$$V_{out} = \frac{1}{1 - D_h} V_{in},$$

Where  $D_b$  is the duty ratio function of boost converter. Therefore, in the boost converter – inverter system,

$$D_b = 1 - \frac{Vin}{V_{out}} = 1 - \frac{V_{in}}{V_{dc}}.$$

Since all the voltage values in above equations are already known or related to output voltage references, the duty ratio function can be calculated and used as feed forward control information for inverter and boost converter. Figure 2.4 and 2.5 shows simulation result for different power factor values using PWAM method for the boost converter – inverter system.

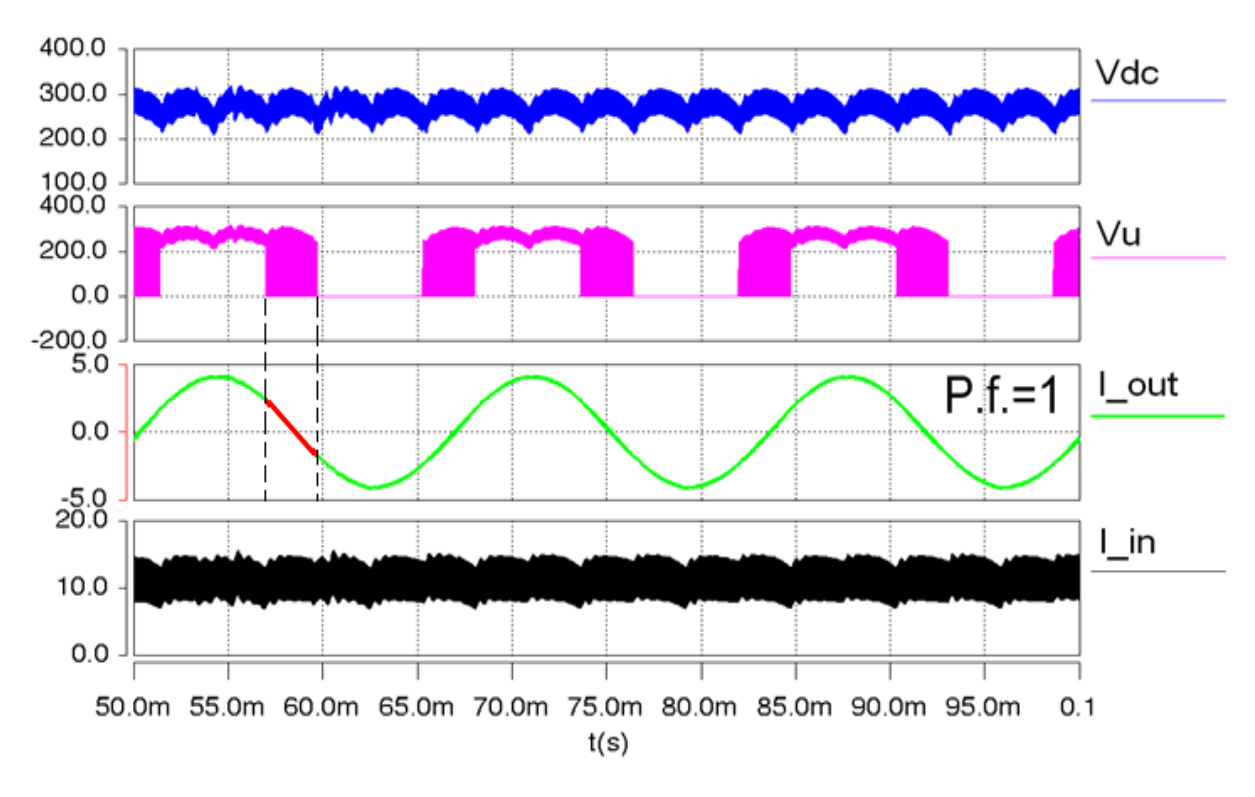


Figure 2.4 PWAM simulation (P.F.=1)

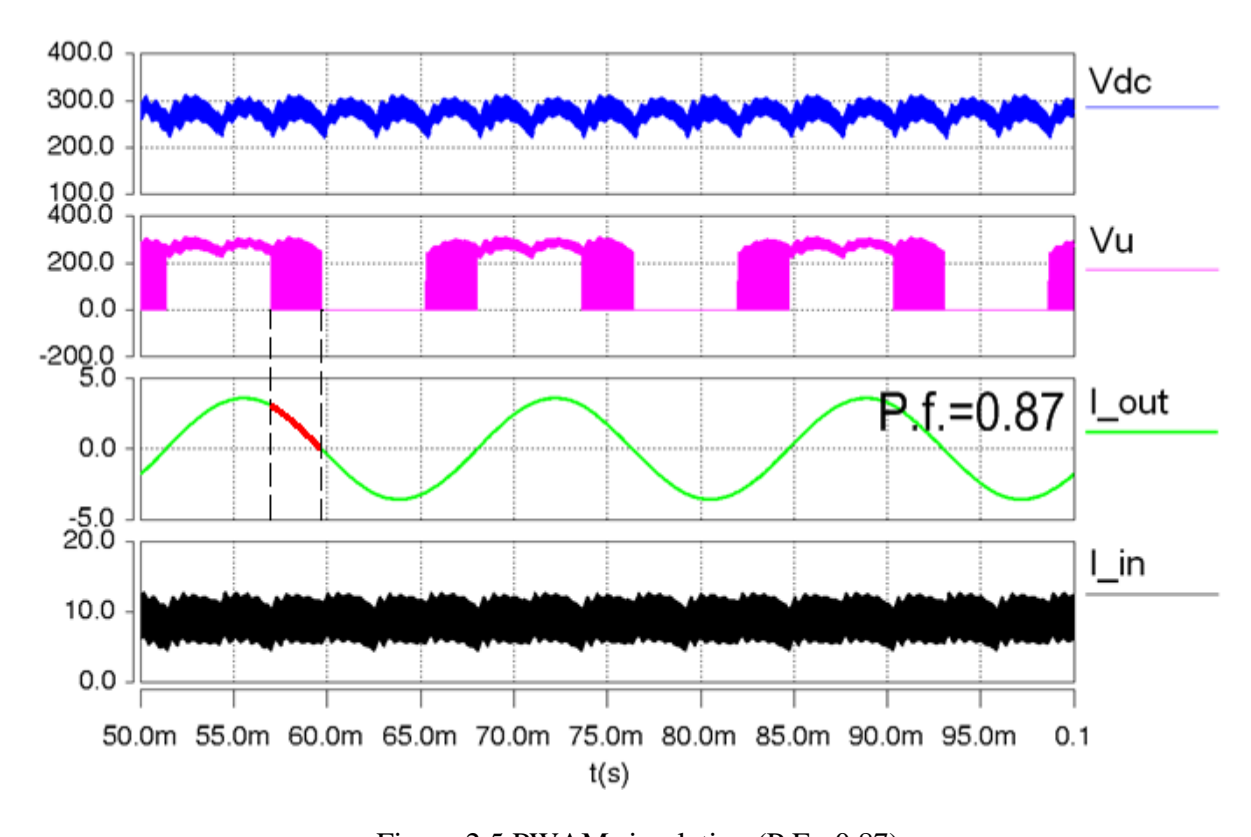


Figure 2.5 PWAM simulation (P.F.=0.87)

# **CHAPTER 3** System Power Losses Analysis

The power losses of the whole system could be caused by several different factors.

- For boost converter, there are device switching loss, conduction loss, the dc inductor copper loss and core loss.
- 2. For the inverter, there are also device switching loss and conduction loss.

The PWAM only has effect on reducing inverter switching loss; theoretically the other parts of system loss should stay the same. In this chapter, power loss analysis focus on the inverter side of the system, and the calculation is based on one type of the IGBT integrated power module (IPM) chip that is already chosen for building system prototype and running efficiency test. More information of the IPM will be given in next chapter.

To show the advantage of PWAM method, power loss analysis is done with a comparison between PWAM and the conventional Sinusoidal PWM (SPWM) method.

## 3.1 Inverter Switching Loss

According to the data sheet information from [], the switching loss per IGBT using conventional SPWM method in the inverter system is

$$P_{SW-SPWM} = f_{SW} \cdot \frac{1}{2\pi} \cdot \int_0^{\pi} (E_{SW(on)} + E_{SW(off)}) dwt.$$

Assuming switching energy loss  $E_{sw(on)}$  and  $E_{sw(off)}$  are variables that change linearly with the product of drain-to-source voltage  $V_{CE}$  and drain current  $i_C$ , which are

$$\frac{E_{on}}{E_{on0}} = \frac{V_{CE} \cdot i_C}{V_{CE0} \cdot I_{C0}}$$

and

$$\frac{E_{off}}{E_{off0}} = \frac{V_{CE} \cdot i_{C}}{V \cdot CE0 \cdot I \cdot C0},$$

Where

$$i_C = I_C \cdot \sin(wt)$$
.

So the switching loss of each IGBT can be represented as

$$P_{SW-SPWM} = \frac{V_{CE} \cdot I_{C} \cdot f_{SW}}{\pi} \cdot (\frac{E_{on0}}{V_{CE0} \cdot I_{C0}} + \frac{E_{off0}}{V_{CE0} \cdot I_{C0}})$$

For the case of PWAM method, figure 2.4 shows the waveform of drain-to-source voltage and collector current when the power factor equals to 1. The output voltage and current are in phase. One of the inverter phase leg is doing PWM switching action while phase current is in the small value region. Since the switching action only happens during the periods  $(-\pi/6, \pi/6)$  and  $(5\pi/6, 7\pi/6)$ , the switching loss can be calculated by

$$\begin{split} &P_{SW-SPWM} \\ &= (E_{SW(on)} + E_{SW(off)}) \cdot [\frac{1}{2\pi} \int_{-\pi/6}^{\pi/6} |\sin(wt)| dwt + \frac{1}{2\pi} \int_{5\pi/6}^{7\pi/6} |\sin(wt)| dwt] \\ &= \frac{2 - \sqrt{3}}{2} \cdot \frac{V_{CE} \cdot I_{C} \cdot f_{SW}}{\pi} \cdot (\frac{E_{on0}}{V_{CE} \cdot I_{C0}} + \frac{E_{off0}}{V_{CE0} \cdot I_{C0}}) \end{split}$$

Therefore, the switching loss of PWAM method is only

$$\frac{P_{SW} - PWAM}{P_{SW} - SPWM} = \frac{2 - \sqrt{3}}{2} = 13.4\%$$

comparing with the conventional SPWM method.

For the inductive load such as a motor, the power factor is not equal to 1 as shown in figure 2.5. Each IGBT switching loss should be expressed as

$$\begin{split} &P_{SW-SPWM} \\ &= (E_{SW(on)} + E_{SW(off)}) \cdot [\frac{1}{2\pi} \int_{-\pi/6}^{\pi/6} |\sin(wt - \theta)| dwt + \frac{1}{2\pi} \int_{5\pi/6}^{7\pi/6} |\sin(wt - \theta)| dwt] \\ &\qquad \qquad (P.F. = \cos \theta) \end{split}$$

In figure 2.5, relatively larger currents flow through the IGBT when the switching action takes place. Switching loss will then increase as the load power factor decreases from 1. This means the most efficient running point for the inverter is at the unit power factor, and the worst case happens when power factor equals to 0. At the point of worst case, switching power loss of PWAM method reaches 50% of the switching loss of SPWM method. That still reduces half of the switching loss for inverter. Figure 3.1 shows the relationship between  $P_{SW-PWAM}/P_{SW-SPWM}$  and power factor.

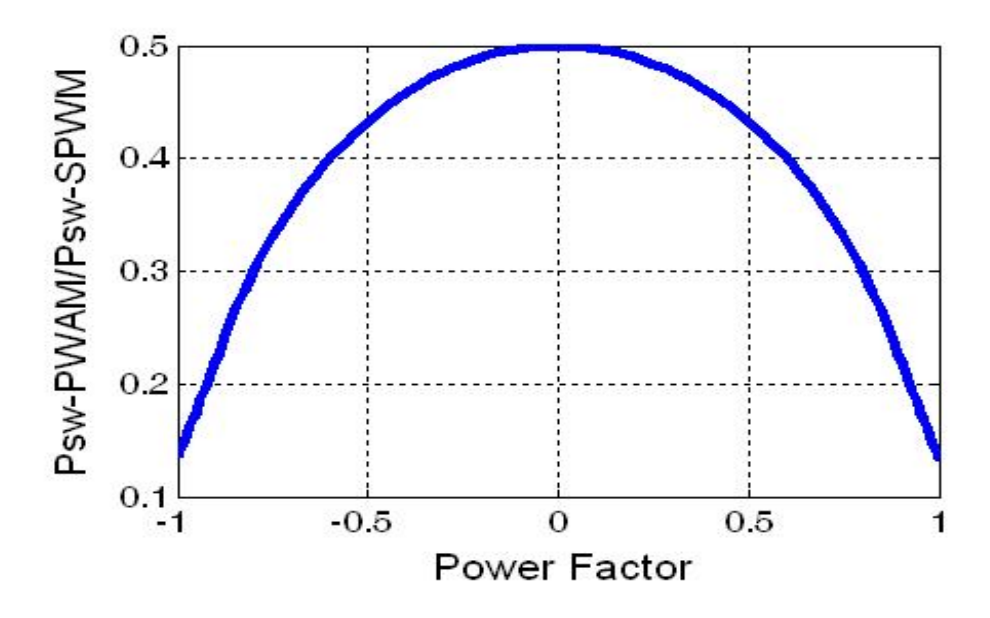


Figure 3.1 The relationship between power loss and load power factor

In addition, the diode recovery loss should be considered in the inverter switching loss calculation as well. During each switching action, the recovery loss per diode can be written as

$$P_D = I_{rr} \cdot t_{rr} \cdot V_{CE} \cdot f_{sw} = Q_{rr} \cdot V_{CE} \cdot f_{sw}$$

Because each phase leg only switches for one third of fundamental period, the recovery loss should be only  $P_D/3$ .

Figure 3.2 shows the switching loss of inverter in terms of different system power rating using PWAM method and SPWM method. All the values regarding to the inverter for loss calculation are from the datasheet. Inverter conduction loss for both control strategies should not have much difference, since the conduction loss is generated from either IGBT switch or the freewheeling diode all the time. On the other hand, switching loss is significantly reduced from 15W (SPWM) to 3W (PWAM).

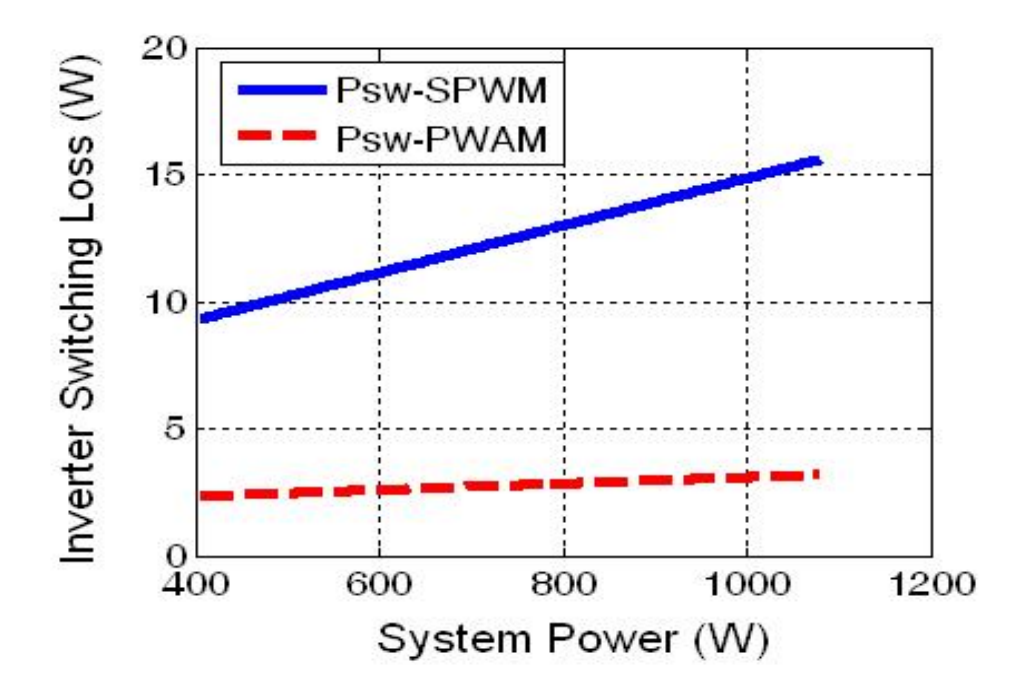


Figure 3.2 Switching loss comparison between PWAM and SPWM

### 3.2 Inverter Conduction Loss

The switching duty ratio D(t) in PWAM method is quite different from the one in SPWM method. If take phase leg "a" as an example, the function of D(t) can be written as:

$$D(t) = \begin{cases} \frac{\cos(wt - \pi/3)}{\cos(wt)}, & wt \in [-\pi/6, \pi/6] \\ 1, & wt \in [\pi/6, 5\pi/6] \\ \frac{\cos(wt + \pi/3)}{\cos(wt)}, & wt \in [5\pi/6, 7\pi/6] \\ 0, & wt \in [7\pi/6, 11\pi/6] \end{cases}$$

From the DIP IPM data sheet,

$$V_{CE} = \frac{1}{12} \cdot I_C + 1 = R_{CE} \cdot I_C + V_{CE0}$$

It can be found

$$V_{CE0} = 1V, R_{CE} = 1/12\Omega$$

Then the conduction loss per switching IGBT can be calculated by

$$V_{cond} = \frac{V_{CE0}}{2\pi} \cdot \int_0^{2\pi} [i_C(t) \cdot D(t)] dwt + \frac{R_{CE}}{2\pi} \cdot \int_0^{2\pi} [i_C^2(t) \cdot D(t)] dwt$$

Since the up switch and the bottom switch in each phase leg always operate at complimentary condition, the inverter conduction loss would be generated all the time either from the up switch or the bottom switch, so there is not a significant difference or change on conduction loss when the PWAM method is applied in the system.

# CHAPTER 4 Experiment Setup/Result and

# **Efficiency Test**

This chapter describes all the hardware work that has been done. A 1-kW experiment prototype of boost converter – inverter system was built. System efficiency was tested with both SPWM and PWAM control method. The advantage of PWAM method on power loss reduction is verified. Some other modifications have also been made to improve system performance.

### 4.1 Experiment Setup and Result

To test system efficiency, a boost converter – inverter prototype was built shown in figure 4.1. The "DSP TMS320F28335" board is a product bought from Texas Instruments. It generates all PWM control signals and sends them to the boost converter – inverter system. The PCB board of the boost converter – inverter system includes every major component except for the dc input inductor, which is placed at the right corner in the picture. "Powerex" 600-V DIPIPM chips were used for both boost converter and inverter. There are 6 IGBT switch devices in each DIPIPM chip module. The current rating for inverter side is 10A, and for boost converter side is 30A. For the dc-link capacitor, two different capacitors was installed specially for different control method, since a fixed dc-link voltage needs to be remained in SPWM, while a fluctuated dc-link voltage is expected in PWAM. Table I lists the system specification for the system.

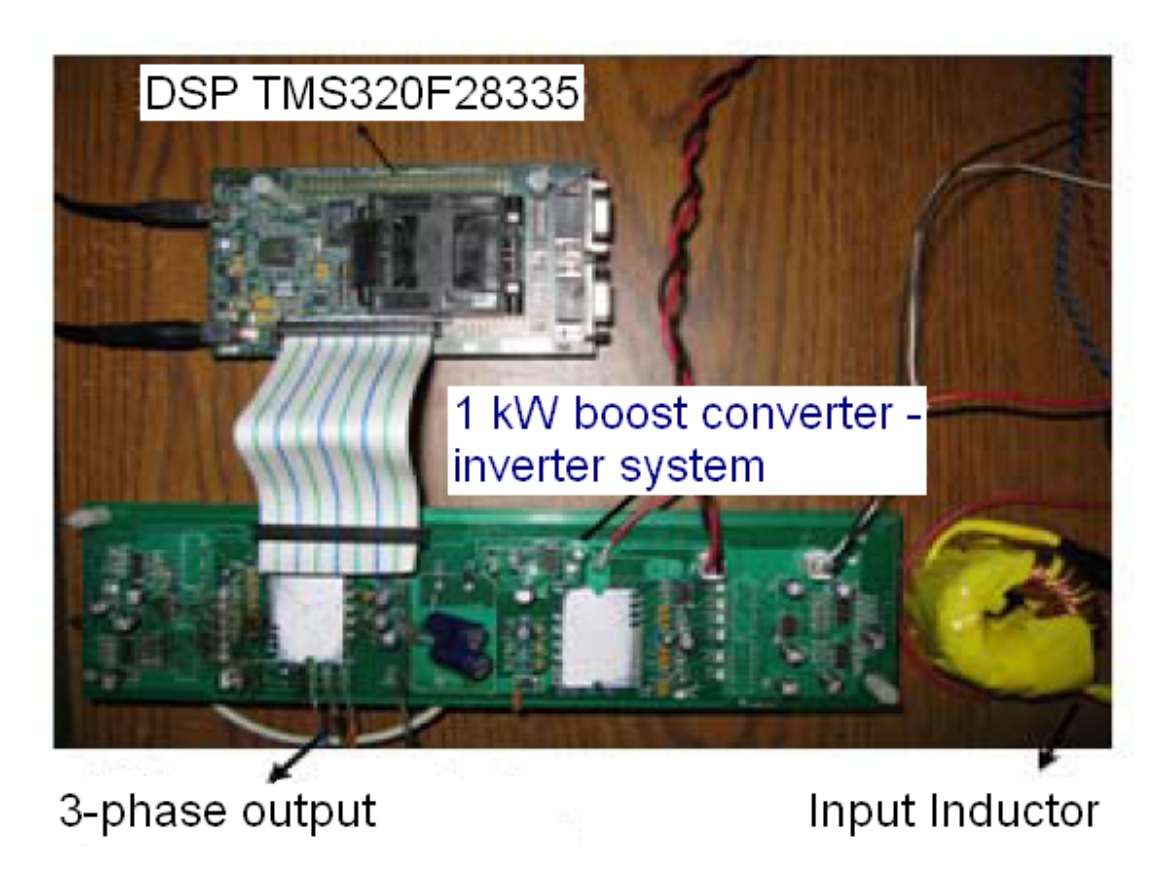


Figure 4.1 Boost converter –inverter system prototype

Table I. System specification for experiment

Output Power	1 kW
Input battery voltage $V_{in}$	100~150 V
DC-link voltage $V_{dc}$	300 V
Output voltage $V_{ll(rms)}$	208 V
Input current $I_{in}$	7~10 A
Output current	3 A
Switching frequency	20 kHz (boost/inverter)
Output frequency	60 Hz or higher
Input inductor $L_{in}$	600 μΗ
DC-link capacitor $C_{dc}$	3 μF (PWAM) / 40 μF (SPWM)

Before taking efficiency test, PWAM method was realized in the system prototype. The working condition of the PWAM method followed the expectation and matched the simulation results shown in chapter 2. Figure 4.2 illustrates voltage VCE of the three lower IGBTs in the three phase leg, and figure 4.3 shows the three phase output voltage and dc-link voltage waveform when system is running at 1kW power level.

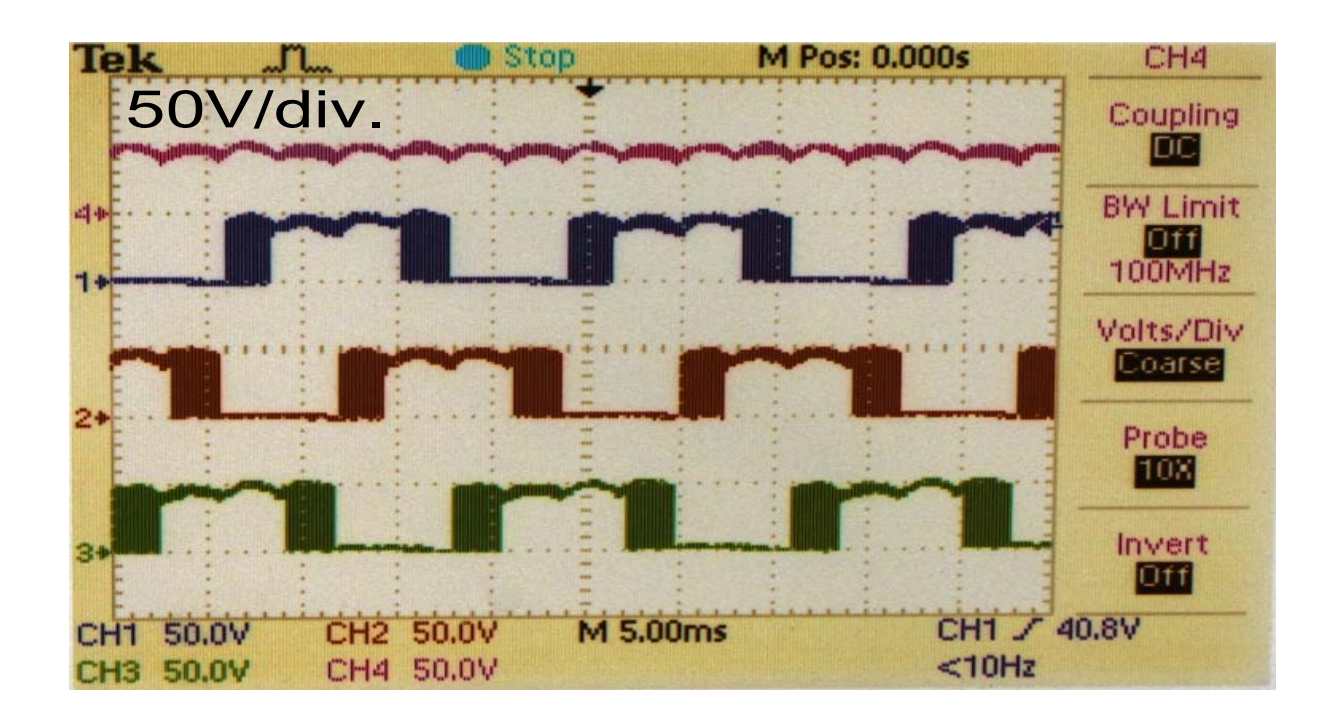


Figure 4.2 DC-link waveform and IGBT voltage waveforms in three phase legs

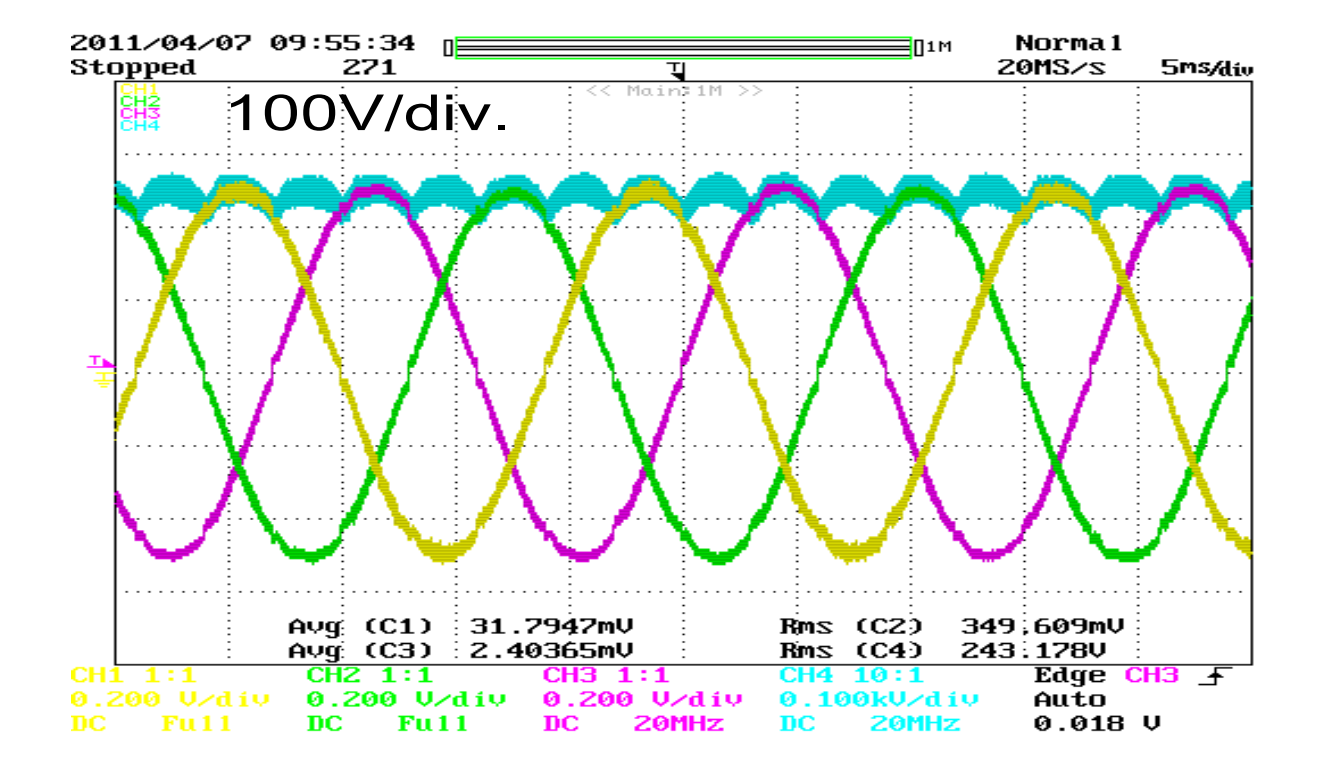


Figure 4.3 DC-link waveform and 3-phase output line-to-line voltage using PWAM at 1 kW

The efficiency tests have been done. Figure 4.4 shows two efficiency curves. The upper curve represents system efficiency for PWAM method. Power loss reduction is obvious. System efficiency could not improve too much because the inverter switching loss is less than 20 W, while inverter conduction loss (about 10 W), power losses in boost converter and input inductor are still not changed.

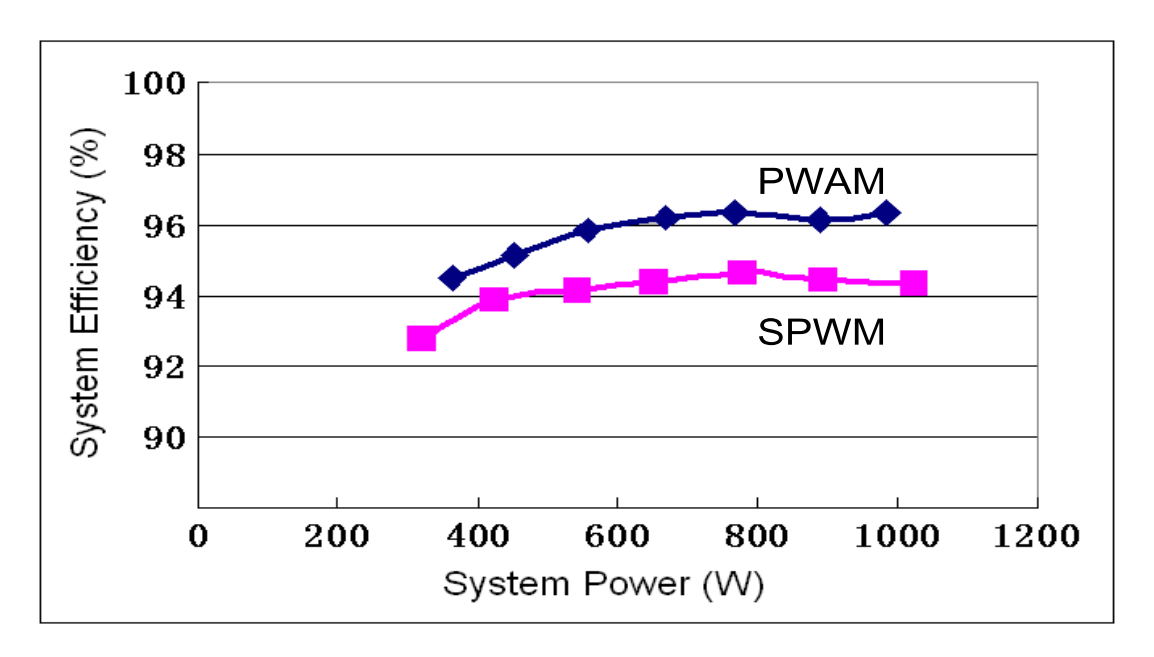


Figure 4.4 Efficiency curves of PWAM and SPWM

## 4.2 System Modifications

The system modifications have been done mainly on two aspects: PCB layout improvement and IGBT IPM chip thermal design.

#### 4.2.1 PCB Layout

The system PCB board design and performance was assessed from the beginning when components was soldered on to the board to the end of efficiency tests. The problems that were found out from the first version of PCB layout are very helpful for design improvement of the second version PCB layout. Figure 4.5 illustrates the system board layout. The DC-DC converter and the DC-AC inverter blocks in the figures represent IPM chips. (a) is the first version and (b) is the second version. A few problems are listed for the (a) and the corresponding modification could be found in (b).

- The shape of (a) is rectangular (27.5 cm by 7.5 cm), it is not strong enough on structure. The body of the board got bent after several months. One the other hand, shape of (b) is close to a square (12.5 cm by 9 cm), it is smaller and stronger. Components on the board are more compact.
- The traces distance of PWM control signals are too long on board (a). It is really important to get clear control signals for the system, this can be achieved by shortening the signals' traces.
- The dc-link capacitor is placed between two IPM chips on the board (a). This is not a good arrangement for thermal design because it is hard to install heat sink for the IPM. On board (b), dc-link capacitor is located by the side of two IPM chips, the room for heat sink has been reserved.
- Some other minor improvements are also considered, for example, small component
   (values of resistors, capacitors) selection and trace width.

Figure 4.6 is the picture that shows the two versions of design of the real PCB boards.

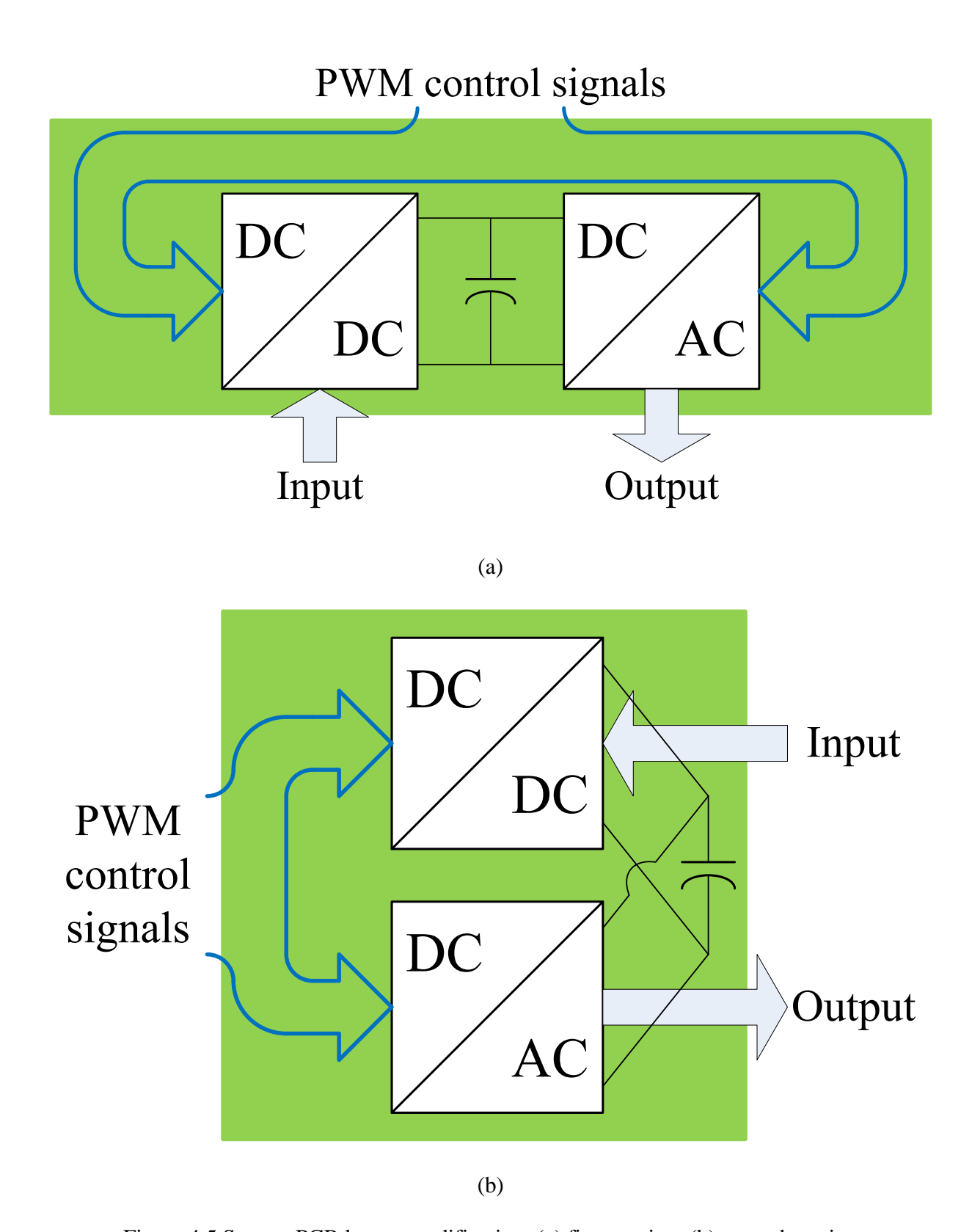
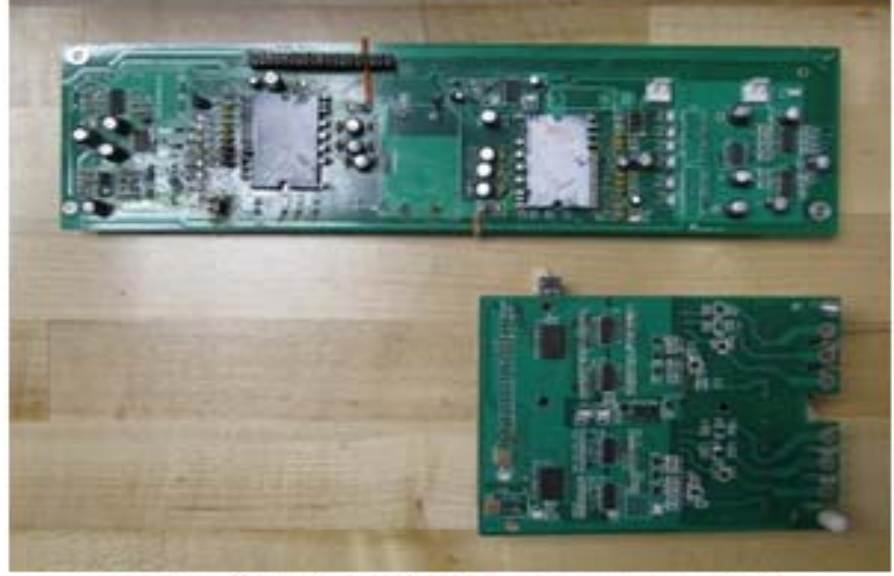


Figure 4.5 System PCB layout modification: (a) first version; (b) second version

Version 1 (27.5 cm x 7.5 cm)



Version 2 (12.5 cm x 9 cm)

Figure 4.6 Version comparison picture

## **CHAPTER 5** Conclusion and future work

### 5.1 Conclusion

In this thesis, a novel control strategy for HEV/EV motor/generator system was introduced. This modulation method requires only one out of three inverter phase legs to do switching action for every PWM carrier period. Switching times thus was greatly reduced by 2/3. According to theoretical analysis, inverter switching loss using PWAM can be as low as 13.4% of the switching loss using SPWM. However, the switching loss reduction of PWAM method varies with different load power factor. To drive electric motor, PWAM method will reduce switching loss by at least 50%, comparing with SPWM.

Unlike the conventional inverter system, which requires relatively larger dc-link capacitor to absorb ripple and keep voltage stable, the system dc-link voltage appears to be fluctuating when PWAM is applied. This is a special feature of PWAM method. Hence, system does not need large dc-link capacitor any more.

### 5.2 Future Work

Lots of work could be planed and executed in the future. First, the system prototype can be further optimized to get even higher efficiency or reducing even more switching loss. The major device in the boost converter – inverter system is the IGBT IPM, but this switching device is not the best option for PWAM method because its switching loss is not dominant part of the total power loss. In this case, there was not a significant power loss reduction or efficiency

improvement for this system. This means PWAM should be applied in a system where the most part of power loss is from switching loss.

In addition, the input dc inductor was not well designed to operate under high efficiency. Beside the loss from switching devices, this inductor could be another source where loss comes from. If all the other system components including the input inductor are well designed, system efficiency also would increase.

Finally, after all the analysis and experiments, limitation of PWAM method is also recognized. As mentioned in previous chapter, the dc-link voltage ripple is needed to be controlled at 6 times of output fundamental frequency, when motor/generator is running at high speed, controlling the dc-link ripple would be much difficult. More investigation could be done about this concern.

Bibliography

# Bibliography

- [1] M. H. Rashid, "Power Electronics Circuits, Devices, and Applications", Third Edition, Person Education Inc., 2004
- [2] "Application Note 4266 An Efficiency Primer for Switch Mode, DC-DC Converter Power Supplies", posted on Dec. 23, 2008, accessed on Dec. 6, 2012, < http://www.maximintegrated.com/app-notes/index.mvp/id/4266>
- [3] H. W. van der Broeck, H. C. Skudelny and G. V. Stanke, "Analysis and Realization of a Pulsewidth Modulator Based on Voltage Space Vectors", *IEEE Transactions on Industry Applications*, 1988, pp. 142-150.
- [4] B. Kaku, I. Miyashita, and S. Sone, "Switching loss minimized space vector PWM method for IGBT three-level inverter", *IEE Proc. Electric Power Applicat.*, vol. 144, no. 3, pp.182-190, 1997.
- [5] J. W. Kolar, H. Ertl, and F. C. Zach, "Influence of the Modulation Method on the Conduction and Switching Losses of a PWM Converter System", *IEEE Transactions on Industry Applications*, Vol. 27, No. 6, pp. 1063-1075, 1991.
- [6] A. M. Hava, R. J. Kerkman and T. A. Lipo, "Simple Analytical and Graphical Methods for Carrier-Based PWM-VSI Drives", *IEEE Transactions on Power Electronics*, 1999, pp. 49-61.
- [7] O. Ojo, "The generalized discontinuous PWM scheme for three-phase voltage source inverters", *IEEE Trans. Ind. Electron.*, vol. 51, no. 6, pp.1280 -1289, 2004.
- [8] A. M. Hava, R. J. Kerkman and T. A. Lipo, "A High Performance Generalized Discontinuous PWM Algorithm", *APEC*, 1997, pp. 886-894.
- [9] Y. Wu, C. Y. Leong and R. A. McMahon, "A Study of Inverter Loss Reduction Using Discontinuous Pulse Width Modulation Techniques", PEMD, 2006, pp. 596-600.
- [10] Y. Wu, M. A. Shafi, A. M. Knight, and R. A. McMahon, "Comparison of the Effects of Continuous and Discontinuous PWM Schemes on Power Losses of Voltage-Sourced Inverters for Induction Motor Drives", *Power Electronics, IEEE Transactions on*, vol.26, no.1, pp.182-191, Jan. 2011.
- [11] C. Y. Leong, R. Grinberg, G. Makrides, Y. Wu and R. A. McMahon, "A comparison of losses in small (<1kW) drives using sine and space vector pulse width modulation schemes", PEDS, 2005, pp. 1123-1128.

- [12] C. Y. Leong, N. P. van der Duijn Schouten, P. D. Malliband and R. A. McMahon, "A Comparison of Power Losses for Small (<1kW) Induction Motor Drives Adopting Squarewave and Sinusoidal PWM Excitation", Second International Conference on Power Electronics, Machines and Drives, 2004, pp. 286-290.
- [13] D. M. Divan, "The resonant dc link converter A new concept in static power conversion", in *Conf. Rec. IEEE IAS Annu. Mtg.*, pp.648-656, 1986.
- [14] D. M. Divan and G. Skibinski, "Zero-switching-loss inverters for high-power applications", *IEEE Trans. Ind. Applicat.*, vol. 25, pp.634 -643, 1989.
- [15] H. Fujita, S. Tominaga and H. Akagi, "A practical approach to switching-loss reduction in a large-capacity static var compensator based on voltage-source inverters", *IEEE Trans. Ind. App.*, vol. 36, no. 5, pp.1396 -1404, 2000.
- [16] J. S. Kim and S. K. Sul, "New control scheme for ac-dc-ac converter without dc link electrolytic capacitor", in *Proc. of the IEEE PESC'93*, 1993, pp. 300-306.
- [17] H. Fujita, "A three-phase voltage-source solar power conditioner using a single-phase PWM control method", in *Energy Conversion Congress and Exposition*, 2009. *ECCE* 2009. *IEEE*, 2009, pp. 3748-3754.
- [18] H. Fujita, "Switching loss analysis of a three-phase solar power conditioner using a single-phase PWM control method", in *Energy Conversion Congress and Exposition (ECCE)*, 2010 IEEE, pp. 618-623.
- [19] Powerex Duel-in-line intelligent power module datasheet: PS21963-4, 10 Amperes/600 Volts